Doppler Shift Tolerance of Accumulation and Outer Coding in MIMO-PMCW Radar

Lucas Giroto de Oliveira, *Graduate Student Member, IEEE*, Elizabeth Bekker, *Graduate Student Member, IEEE*, Akanksha Bhutani, *Member, IEEE*, Axel Diewald, *Graduate Student Member, IEEE*, Benjamin Nuss, *Graduate Student Member, IEEE*, Theresa Antes, and Thomas Zwick, *Fellow, IEEE*

***Abstract*— Phase-modulated continuous wave (PMCW) has been widely regarded as a promising modulation scheme for radar systems, e.g., in highly automated driving (HAD) applications. Although the so-called outer coding can efficiently enable the multiple-input–multiple-output (MIMO) operation of PMCW-based radar systems, the yielded processing gain in this multiplexing approach may be reduced at increasing Doppler shifts. In this context, this letter introduces a normalized Doppler shift parameter that enables predicting the Doppler-shift-induced degradation of the processing gain in a MIMO-PMCW radar system. Finally, simulation and measurement results confirm the usefulness of the introduced parameter in desigining MIMO-PMCW radars.**

***Index Terms*— Doppler-shift tolerance, multiple-input–multiple-output (MIMO), outer coding, phase-modulated continuous wave (PMCW), radar sensing.**

I. Introduction

In THE context of highly automated driving (HAD), phase-modulated continuous wave (PMCW) appears as an attractive alternative to enable efficient digital radar sensing [1]–[3] and radar-communication (RadCom) operation [4]–[8] at the cost of moderate hardware requirements [9] compared to, e.g., orthogonal frequency-division multiplexing (OFDM) [10], [11], while also posing high data rate and storage requirements [12].

To enable multiple-input–multiple-output (MIMO) operation and consequently direction of arrival (DoA) estimation [13], PMCW radar systems can, e.g., use orthogonal pseudorandom binary sequences (PRBSs) [8], [14]–[16] or encode the same PRBS with distinct codewords at each transmit channel [8], [14], [15], [17]. While the first approach yields poor isolation [15], the latter attains a high level of isolation among perfectly synchronized transmit channels at low to moderate Doppler shifts. However, the need for multiple PRBS repetitions to obtain a single range profile in this scheme may result in a noncoherent sum of PRBS repetitions during both accumulation and decoding due to Doppler-shift-induced phase rotations. In this sense, not only the maximum unambiguous velocity must be constrained while parameterizing a MIMO-PMCW radar system but also the Doppler shift tolerance of accumulation and decoding must be considered. This letter addresses this issue by introducing a normalized Doppler shift parameter that takes into account key aspects of a MIMO-PMCW radar system independently of the adopted PRBS. This enables a straightforward prediction of the resulting degradation of the processing gain of accumulation and decoding.

Manuscript received June 30, 2021; revised September 15, 2021; accepted October 4, 2021. This work was supported by the Federal Ministry of Education and Research (BMBF), Germany, through the Project "ForMikro-REGGAE," under Grant 16ES1061. The work of Lucas Giroto de Oliveira was supported by the German Academic Exchange Service (DAAD)–Funding Program under Grant 57440921/Pers. Ref. No. 91555731. *(Corresponding author: Lucas Giroto de Oliveira.)*

The authors are with the Institute of Radio Frequency Engineering and Electronics (IHE), Karlsruhe Institute of Technology (KIT), 76131 Karlsruhe, Germany (e-mail: lucas.oliveira@kit.edu).

Color versions of one or more figures in this letter are available at https://doi.org/10.1109/LMWC.2021.3123691.

Digital Object Identifier 10.1109/LMWC.2021.3123691

II. MIMO-PMCW Radar System Model

Let a MIMO radar system consist of an in-band full duplex (IBFD) radio frequency (RF) device, in which orthogonal PMCW signals are transmitted by $P \in \mathbb{N}_+$ transmit antennas and reflections off targets are captured by $Q \in \mathbb{N}_+$ receive antennas. In this system, each transmit signal consists of weighted repetitions of a N_{PRBS}-length binary PRBS, $N_{\text{PRBS}} \in \mathbb{N}_+$, with a chip or sampling rate of F_s samples per second that modulate a carrier of frequency $f_\text{c} \gg F_\text{s}$.

To ensure orthogonality among the P transmit signals, outer coding is adopted [8], [14], [15], [17]. Consequently, each transmit channel transmits P coded sets of $A \in \mathbb{N}_+ | A > 1$ repetitions of the adopted PRBS to ultimately generate a single range profile after radar signal processing at the receiver side. The resulting sequence from the P coded sets is henceforth called a block. In this context, the encoding at the pth transmit channel in the considered outer-coding-based MIMO scheme consists of multiplying each of the P aforementioned sets by its respective element of the Hadamard codeword $\mathbf{c}^p \in \{-1, 1\}^{P\times 1}$, $p \in \{0, 1, \ldots, P-1\}$. The codewords $\mathbf{c}^p$ are defined such that ${\mathbf{c}^{p_1}}^T \mathbf{c}^{p_2} = P \;\forall\; p_1 = p_2$ and ${\mathbf{c}^{p_1}}^T \mathbf{c}^{p_2} = 0 \;\forall\; p_1 \neq p_2$ for $p_1, p_2 \in \{0, 1, \ldots, P-1\}$, and can be simply extracted from the pth row of the Hadamard matrix $\mathbf{C} \in \{-1, 1\}^{P\times P}$, which requires $\text{mod}\,(P, 4) = 0$ for $P > 2$ and, typically, that P, $P/12$, or $P/20$ is a power of 2. Assuming that the aforementioned constraints are satisfied in the considered MIMO-PMCW radar system, the A repetitions of the adopted PRBS in each of the P PRBS blocks are required for two reasons: 1) to increase the signal-to-noise ratio (SNR) via accumulation at the receiver and 2) to enable compensation for eventual phase breaks between consecutive blocks weighted by different elements of $\mathbf{c}^p$. The aforementioned compensation consists of discarding the first

out of each A PRBS repetitions in each block [8], [17] similar to the cyclic prefix (CP) principle in OFDM [18].

Without loss of generality, it is assumed that a single block is transmitted. Omitting power factors, the discrete-time domain sequence $x^p[\eta] \in \mathbb{C}$, containing the block of the pth transmit channel, is expressed for $\eta \in \{0, 1, \ldots, PAN_{\text{PRBS}} - 1\}$ as in (1), shown at the bottom of the page. There, $c_{\varpi}^{p} \in \{-1, 1\}$ is the ϖth element of $\mathbf{c}^p$, $\varpi \in \{0, 1, \ldots, P-1\}$. Additionally, $\psi[n] \in \{-1, 1\}$ is the PRBS defined for $n \in \{0, 1, \ldots, N_{\text{PRBS}} - 1\}$, and rect($\xi$) is the rectangular function taking the value 1 for $\xi \in [0, 1)$ and 0 otherwise. After digital-to-analog (D/A) conversion on $x^p[\eta]$, the resulting continuous-time domain signal undergoes analog conditioning, up-conversion to the carrier frequency f_{c}, and transmission by the pth transmit antenna. Next, it is without loss of generality considered that the resulting signal is reflected off a single point target that has range $R^{q,p}$ and relative radial velocity $v^{q,p}$ w.r.t. the pth transmit and qth, $q \in \{0, 1, \ldots, Q-1\}$, receive antennas. The captured reflection by the qth receive antenna undergoes analog conditioning and analog-to-digital (A/D) conversion in an I/Q receiver, resulting in the sequence $y^q[\eta] \in \mathbb{C}$ as in (2), shown at the bottom of the page. In this equation, $\alpha^{q,p}$ is the attenuation factor defined by the antenna gains, radar cross section (RCS) of the point target, and the propagation loss experienced in the overall traveled path of length $R^{q,p}$ from the pth transmit antenna to the point target and back to the qth receive antenna. Furthermore, c_0 denotes the speed of light in vacuum in meters per second, and $f_{\text{D}}^{q,p} = 2v^{q,p}/\lambda_{\text{c}}$ (with $\lambda_{\text{c}} = c_0/f_{\text{c}}$ denoting the carrier wavelength) is the Doppler shift induced in the signal reflecting off the point target. Moreover, $\phi^{q,p} \in \mathbb{R} | \phi_h^{q,p} = -2\pi(R^{q,p}/\lambda_{\text{c}})$ is the carrier phase associated with the pth transmit and qth receive channels and the point target, which is exploited for DoA estimation. Finally, $z[\eta]$ is the additive white Gaussian noise (AWGN). Further typical processing steps to yield a single range profile associated with the pth transmit and qth receive channels in the MIMO-PMCW radar system comprise: serial-to-parallel (S/P) conversion, accumulation of $A-1$ out of each A PRBS repetitions, decoding, and correlation with the adopted PRBS.

An important aspect in the MIMO-PMCW radar system is their robustness to Doppler shifts, which induce the following impairments: 1) degradation of both main lobe and sidelobe levels of the obtained range profile via correlation with the adopted PRBS [16] and 2) noncoherent sum of sequence repetitions during accumulation and decoding. The first effect depends on the adopted PRBS and is therefore not discussed in further detail. This letter focuses on the latter impairment, which is independent of the chosen PRBS. In this sense, the resulting vector $\mathbf{r}^{q,p} \in \mathbb{C}^{N_{\text{PRBS}} \times 1}$ from S/P conversion, accumulation, and decoding with the codeword $\mathbf{c}^p$, associated with the pth transmit channel, on $y^q[\eta]$ has its nth element $r_n^{q,p}$ as expressed in (3), shown at the bottom of the page. An analysis of this equation reveals that the yielded processing gain via accumulation and decoding is

$$G_{\text{p}} = \frac{\left| \sum_{\varpi=0}^{P-1} \sum_{a=1}^{A-1} \text{e}^{\text{j}2\pi f_{\text{D}}^{q,p}(aN_{\text{PRBS}} + \varpi AN_{\text{PRBS}})/F_{\text{s}}} \right|^2}{P(A-1)} \tag{4}$$

for any adopted PRBS. The absolute value of the sum of complex exponentials in (4) yields a maximum value of $P(A-1)$ when all complex exponentials add coherently, which only happens for $f_{\text{D}}^{q,p} = 0$ Hz. Furthermore, the numerator and denominator of (4) represent the factors by which accumulation and decoding increase the power of the signal and the AWGN contributions, respectively, of (3) w.r.t. their counterparts in (2). In this context, Section III introduces a normalized Doppler shift parameter, through which the degradation of G_{p} can be predicted.

III. Numerical and Measurement Results

To perform a generic Doppler shift tolerance analysis, a similar parameter to the frequency resolution in OFDM-based systems [8], [19] is used. For PMCW, it is redefined as

$$\Delta f \triangleq F_{\text{s}}/N_{\text{PRBS}} \tag{5}$$

or $\Delta f \triangleq 1/T_{\text{PRBS}}$, where $T_{\text{PRBS}} = N_{\text{PRBS}}/F_{\text{s}}$ is the time duration in seconds of a single PRBS repetition.

Fig. 1(a)–(d) presents the simulated degradation of G_{p} due to Doppler shifts w.r.t. its maximum achievable value $P(A-1)$ for different combinations of repetitions for accumulation and numbers of transmit channels, i.e., $A \in \{2, 16, 128, 1024\}$, $P \in \{2, 4, 8, 16\}$. The normalization of Doppler shifts f_{D} by $\Delta f/(PA)$ in the horizontal axis is due to the time duration of $T_{\text{block}} = PAN_{\text{PRBS}}/F_{\text{s}} = PA/\Delta f$ in seconds of a block. In all cases, very similar Doppler-shift-dependent degradations of G_{p} are experienced, with slight deviations when both P and A are small. It is worth highlighting that the MIMO-PMCW radar system with increasing P and A values experience higher degradations of G_{p} in terms of absolute Doppler shift values f_{D} in comparison to an almost identical degradation when looking at normalized Doppler shifts $f_{\text{D}}/[\Delta f/(PA)]$. Nevertheless, increasing P and A values tend to yield higher G_{p}, in particular for slow-moving targets since $G_{\text{p}} \to P(A-1)$ for $f_{\text{D}} \to 0$ according to (4). The deviations in the processing gain degradations in Fig. 1 are explained by the need to discard

$$x^p[\eta] = \sum_{\varpi=0}^{P-1} c_{\varpi}^{p} \sum_{a=0}^{A-1} \psi[\eta'] \, \text{rect}\left(\frac{\eta'}{N_{\text{PRBS}}}\right), \quad \eta' = \eta - aN_{\text{PRBS}} - \varpi AN_{\text{PRBS}} \tag{1}$$

$$y^q[\eta] \approx \sum_{p=0}^{P-1} \alpha^{q,p} \, x^p\left[\eta - \frac{F_{\text{s}} R^{q,p}}{c_0}\right] \text{e}^{\text{j}2\pi f_{\text{D}}^{q,p} \eta/F_{\text{s}}} \, \text{e}^{\text{j}\phi^{q,p}} + z[\eta] \tag{2}$$

$$r_n^{q,p} \approx \alpha^{q,p} \, \psi\left[n - \frac{F_{\text{s}} R^{q,p}}{c_0}\right] \text{e}^{\text{j}\phi^{q,p}} \sum_{\varpi=0}^{P-1} \sum_{a=1}^{A-1} \text{e}^{\text{j}2\pi f_{\text{D}}^{q,p} n'/F_{\text{s}}} + \sum_{\varpi=0}^{P-1} c_{\varpi}^{p} \sum_{a=1}^{A-1} z[n'], \quad n' = n + aN_{\text{PRBS}} + \varpi AN_{\text{PRBS}} \tag{3}$$

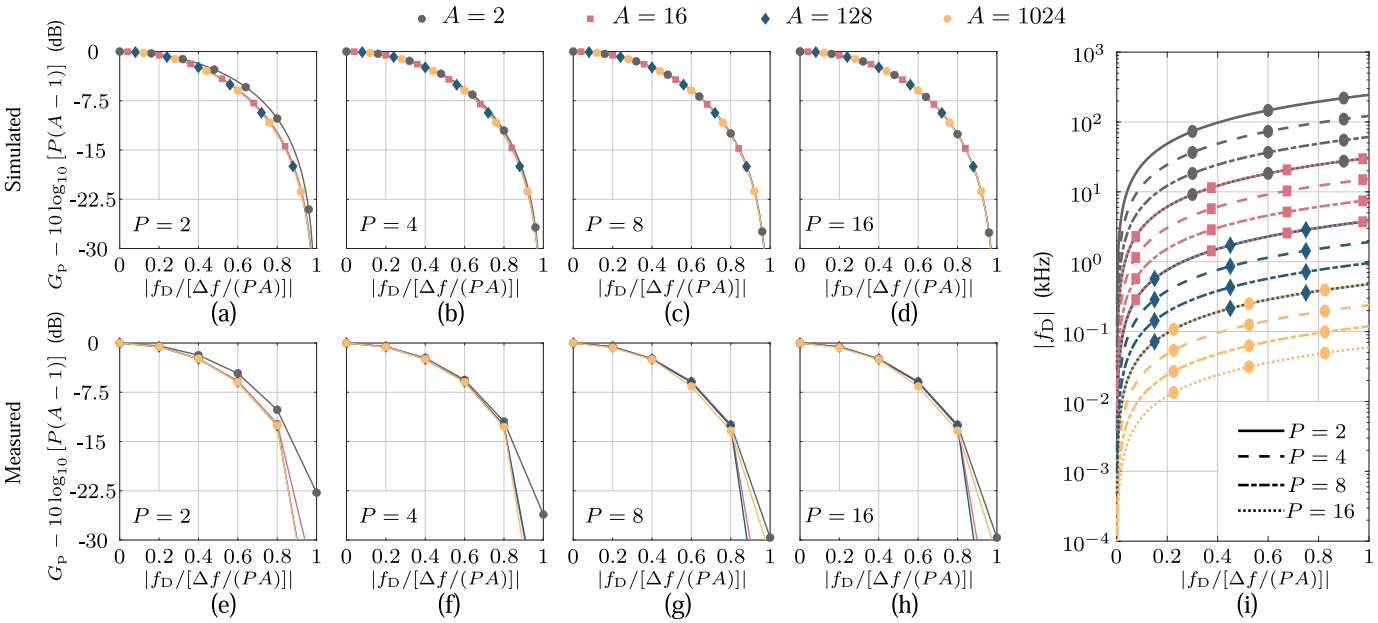

Fig. 1. Degradation of the processing gain for different combinations of the number of transmit channels P and repetitions for accumulation A: simulated for (a) $P = 2$, (b) $P = 4$, (c) $P = 8$, and (d) $P = 16$, and measured (at $|f_\mathrm{D}/[\Delta f/(PA)]| \in \{0, 0.2, 0.4, 0.6, 0.8, 1\}$) for (e) $P = 2$, (f) $P = 4$, (g) $P = 8$, and (h) $P = 16$. In all cases, a good agreement between simulated and measured degradation of G_p is observed. The divergences at $|f_\mathrm{D}/[\Delta f/(PA)]| = 1$ can be explained by the severe degradation of the processing gain and measurement noise. The corresponding Doppler shifts to the normalized axes in the previous subfigures for $F_\mathrm{s} = 1$ GHz and $N_\mathrm{PRBS} = 1023$ and different P and A pairs are shown in (i).

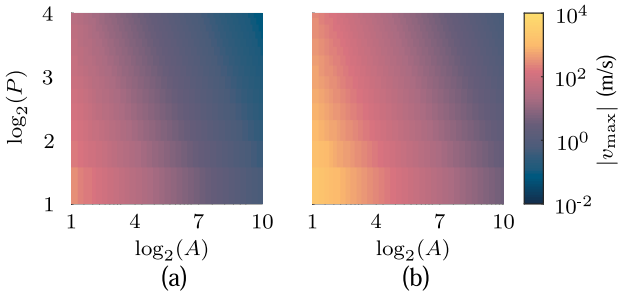

Fig. 2. Maximum tolerable relative radial velocity for $\gamma = 0.6$ in (a) automotive and (b) gesture recognition scenarios.

the first out of each A PRBS repetitions, which according to (4) becomes negligible for higher P and A values. To validate the simulations, measurement results obtained via emulation of a MIMO-PMCW radar system and the radar target simulator (RTS) described in [20]–[23] on Xilinx's Zynq UltraScale+ RFSoC ZCU111 are shown in Fig. 1(e)–(h).

To constrain the degradation of G_p, an upper bound $\gamma \in \mathbb{R}_{\geq 0}$ on the normalized Doppler shift must be defined so that

$$\left|f_\mathrm{D,max}/[\Delta f/(PA)]\right| < \gamma \tag{6}$$

where $f_\mathrm{D,max}$ is the Doppler shift of highest tolerable absolute value. As an example, one must adopt $\gamma = 0.45$ if a G_p degradation of up to 3 dB can be tolerated. To illustrate this condition, Fig. 2 shows the relative radial velocity $v_\mathrm{max} = f_\mathrm{D,max}\,\lambda_\mathrm{c}/2$ associated with the tolerable $|f_\mathrm{D}/[\Delta f/(PA)]|$ ratio in the contexts of automotive and gesture recognition applications. For the first MIMO-PMCW radar system, $F_\mathrm{s} = 1$ GHz and $f_\mathrm{c} = 79$ GHz were adopted, which results in the range resolution $\Delta R = 0.15$ m, while $F_\mathrm{s} = 12.5$ GHz and $f_\mathrm{c} = 140$ GHz were adopted for the latter, yielding $\Delta R = 0.01$ m. A maximum-length sequence (MLS) with length $N_\mathrm{PRBS} = 1023$ was used in both cases, resulting in maximum unambiguous ranges $R_\mathrm{max,unamb} = 153.45$ m and $R_\mathrm{max,unamb} = 12.28$ m for the automotive and gesture recognition scenarios, respectively. Typical further parameterization for the automotive scenario includes $P = 4$, $A = 4$, and a total of $M = 1024$ blocks, resulting in the maximum unambiguous relative radial velocity $|v_\mathrm{max,unamb}| = 57.96$ m/s and the relative radial velocity resolution $\Delta v = 0.11$ m/s. With $\gamma = 0.45$, the maximum tolerable relative radial velocity is calculated as $|v_\mathrm{max,tol}| = 52,17$ m/s, which is lower than the maximum unambiguous relative radial velocity and therefore imposes a further velocity constraint to the system. In the gesture recognition context, $P = 4$, $A = 128$, and $M = 256$ blocks are used, which yields $|v_\mathrm{max,unamb}| = 12.78$ m/s and $\Delta v = 0.10$ m/s. In this case, $\gamma = 0.45$ results in $|v_\mathrm{max,tol}| = 11.50$ m/s, which is, as in the automotive case, lower than $|v_\mathrm{max,unamb}|$.

IV. Conclusion

This letter discussed the Doppler shift tolerance of accumulation and outer coding in the MIMO-PMCW radar system. After deriving a closed-form expression of the effective processing gain at a given Doppler shift, a normalized Doppler shift by key parameters of the MIMO-PMCW radar system was introduced. Based on this normalization, virtually the same degradation of the processing gain was observed for all considered combinations of numbers of PRBS repetitions for accumulation and outer coding. Consequently, the proposed parameter directly relates the number of PRBS repetitions and the degradation of the processing gain, allowing a straightforward prediction of the latter.

REFERENCES

[1] G. Hakobyan and B. Yang, "High-performance automotive radar: A review of signal processing algorithms and modulation schemes," *IEEE Signal Process. Mag.*, vol. 36, no. 5, pp. 32–44, Sep. 2019.

[2] F. Roos, J. Bechter, C. Knill, B. Schweizer, and C. Waldschmidt, "Radar sensors for autonomous driving: Modulation schemes and interference mitigation," *IEEE Microw. Mag.*, vol. 20, no. 9, pp. 58–72, Sep. 2019.

[3] C. Waldschmidt, J. Hasch, and W. Menzel, "Automotive radar—From first efforts to future systems," *IEEE J. Microw.*, vol. 1, no. 1, pp. 135–148, Jan. 2021.

[4] C. Davis, M. Hegde, W. E. Stark, A. Eshraghi, M. Goldenberg, and M. Ali, "Vehicle radar system with a shared radar and communication system," WO Patent 2017 187 331 A1, Nov. 2, 2017. [Online]. Available: https://patentscope.wipo.int/search/en/detail.jsf?docId=WO2017187331

[5] S. H. Dokhanchi, M. R. B. Shankar, Y. A. Nijsure, T. Stifter, S. Sedighi, and B. Ottersten, "Joint automotive radar-communications waveform design," in *Proc. IEEE 28th Annu. Int. Symp. Pers., Indoor, Mobile Radio Commun. (PIMRC)*, Oct. 2017, pp. 1–7.

[6] S. H. Dokhanchi, B. S. Mysore, K. V. Mishra, and B. Ottersten, "A mmWave automotive joint radar-communications system," *IEEE Trans. Aerosp. Electron. Syst.*, vol. 55, no. 3, pp. 1241–1260, Jun. 2019.

[7] K. V. Mishra, M. R. B. Shankar, V. Koivunen, B. Ottersten, and S. A. Vorobyov, "Toward millimeter-wave joint radar communications: A signal processing perspective," *IEEE Signal Process. Mag.*, vol. 36, no. 5, pp. 100–114, Sep. 2019.

[8] L. Giroto de Oliveira, B. Nuss, M. B. Alabd, A. Diewald, M. Pauli, and T. Zwick, "Joint radar-communication systems: Modulation schemes and system design," *IEEE Trans. Microw. Theory Techn.*, pp. 1–31, 2021.

[9] V. Giannini *et al.*, "A 79 GHz phase-modulated 4 GHz-BW CW radar transmitter in 28 nm CMOS," *IEEE J. Solid-State Circuits*, vol. 49, no. 12, pp. 2925–2937, Dec. 2014.

[10] C. Sturm, Y. L. Sit, M. Braun, and T. Zwick, "Spectrally interleaved multi-carrier signals for radar network applications and multi-input multi-output radar," *IET Radar Sonar Navigat.*, vol. 7, no. 3, pp. 261–269, Mar. 2013.

[11] Y. L. Sit, B. Nuss, and T. Zwick, "On mutual interference cancellation in a MIMO OFDM multiuser radar-communication network," *IEEE Trans. Veh. Technol.*, vol. 67, no. 4, pp. 3339–3348, Apr. 2018.

[12] B. Schweizer *et al.*, "The fairy tale of simple all-digital radars: How to deal with 100 Gbit/s of a digital millimeter-wave MIMO radar on an FPGA [application notes]," *IEEE Microw. Mag.*, vol. 22, no. 7, pp. 66–76, Jul. 2021.

[13] C. Vasanelli *et al.*, "Calibration and direction-of-arrival estimation of millimeter-wave radars: A practical introduction," *IEEE Antennas Propag. Mag.*, vol. 62, no. 6, pp. 34–45, Dec. 2020.

[14] D. Guermandi *et al.*, "A 79-GHz 2 × 2 MIMO PMCW radar SoC in 28-nm CMOS," *IEEE J. Solid-State Circuits*, vol. 52, no. 10, pp. 2613–2626, Oct. 2017.

[15] *Millimeter-Wave Radar SoC Integration in CMOS* (The Cambridge RF and Microwave Engineering Series). Cambridge, U.K.: Cambridge Univ. Press, 2019, pp. 162–192.

[16] J. Overdevest, F. Jansen, F. Uysal, and A. Yarovoy, "Doppler influence on waveform orthogonality in 79 GHz MIMO phase-coded automotive radar," *IEEE Trans. Veh. Technol.*, vol. 69, no. 1, pp. 16–25, Jan. 2020.

[17] A. Bourdoux, U. Ahmad, D. Guermandi, S. Brebels, A. Dewilde, and W. Van Thillo, "PMCW waveform and MIMO technique for a 79 GHz CMOS automotive radar," in *Proc. IEEE Radar Conf. (RadarConf)*, May 2016, pp. 1–5.

[18] T. Hwang, C. Yang, G. Wu, S. Li, and G. Y. Li, "OFDM and its wireless applications: A survey," *IEEE Trans. Veh. Technol.*, vol. 58, no. 4, pp. 1673–1694, May 2009.

[19] B. Nuss, J. Mayer, and T. Zwick, "Limitations of MIMO and multi-user access for OFDM radar in automotive applications," in *IEEE MTT-S Int. Microw. Symp. Dig.*, Apr. 2018, pp. 1–4.

[20] A. Diewald *et al.*, "Radar target simulation for vehicle-in-the-loop testing," *Vehicles*, vol. 3, no. 2, pp. 257–271, May 2021.

[21] A. Diewald, B. Nuss, M. Pauli, and T. Zwick, "Arbitrary angle of arrival in radar target simulation," *IEEE Trans. Microw. Theory Techn.*, early access, Aug. 31, 2021.

[22] A. Diewald, T. Antes, B. Nuss, and T. Zwick, "Implementation of range Doppler migration synthesis for radar target simulation," in *Proc. IEEE 93rd Veh. Technol. Conf.*, Apr. 2021, pp. 1–5.

[23] A. Diewald, T. Antes, B. Nuss, M. Pauli, and T. Zwick, "Range Doppler migration synthesis for realistic radar target simulation," in *Proc. IEEE Topical Conf. Wireless Sensors Sensor Netw. (WiSNeT)*, Jan. 2021, pp. 56–58.